Achieving quantum-limited optical resolution

Martin Paúr,[1] Bohumil Stoklasa,[1] Zdenek Hradil,[1] Luis L. Sánchez-Soto,[2,3] and Jaroslav Rehacek[1]

[1]*Department of Optics, Palacky University, 17. listopadu 12, 771 46 Olomouc, Czech Republic*
[2]*Departamento de Óptica, Facultad de Física, Universidad Complutense, 28040 Madrid, Spain*
[3]*Max-Planck-Institut für die Physik des Lichts, Günther-Scharowsky-Straße 1, Bau 24, 91058 Erlangen, Germany*

We establish a simple method to assess the quantum Fisher information required for resolving two incoherent point sources with an imaging system. The resulting Cramér-Rao bound shows that the standard Rayleigh limit can be surpassed by suitable coherent measurements. We explicitly find these optimal strategies and present a realization for Gaussian and slit apertures. This involves a projection onto the optimal bases that is accomplished with digital holographic techniques and is compared with a CCD position measurement. Our experimental results unequivocally confirm unprecedented sub-Rayleigh precision.

arXiv:1606.08332v1 [quant-ph] 27 Jun 2016

Optical resolution is a measure of the ability of an imaging system to resolve spatial details in a signal. As realized long ago [1], this resolution is fundamentally determined by diffraction, which smears out the spatial distribution of light so that point sources map onto finite spots at the image plane. This information is aptly encompassed by the point-spread function (PSF) [2].

The diffraction limit was deemed an unbreakable rule, nicely epitomized by the time-honored Rayleigh criterion [3]: points can be resolved only if they are separated by at least the spot size of the PSF of the imaging system.

The conventional means by which one can circumvent this obstruction are to reduce the wavelength or to build higher numerical-aperture optics, thereby making the PSF narrower. In recent years, though, several intriguing approaches have emerged that can break this rule under certain special circumstances [4–10]. Despite their success, these techniques are often involved and require careful control of the source, which is not always possible in every application.

Quite recently, a groundbreaking proposal [11–13] has reexamined this question from the alternative perspective of quantum metrology. The chief idea is to use the quantum Fisher information to quantify how well the separation between two poorly resolved incoherent point sources can be estimated. The associated quantum Cramér-Rao lower bound (qCRLB) gives a fair bound of the accuracy of that estimation. Surprisingly enough, the qCRLB maintains a fairly constant value for any separation of the sources, which implies that the Rayleigh criterion is secondary to the problem at hand.

In this Letter, we elaborate on this issue presenting quite a straightforward way of determining the quantum Fisher information. More importantly, we find the associated optimal measurement schemes that attain the qCRLB. We study examples of Gaussian and sinc PSFs, and implement our new method in a compact and reliable setup. For distances below the Rayleigh limit, the uncertainty of this measurement is much less than with direct imaging.

Let us first set the stage for our simplified model. We follow Lord Rayleigh's lead and assume quasimonochromatic paraxial waves with one specified polarization and one spatial dimension, x denoting the image-plane coordinate. To facilitate possible generalizations, we phrase what follows in a quantum parlance. A coherent wave of complex amplitude $U(x)$ can thus be assigned to a ket $|U\rangle$, such that $U(x)=\langle x|U\rangle$, where $|x\rangle$ is a vector describing a point-like source located at x.

Moreover, we consider a spatially-invariant unit-magnification imaging system characterized by its PSF, which represents its normalized intensity response to a point light source. We shall denote this PSF as $I(x)=|\langle x|\psi\rangle|^2=|\psi(x)|^2$.

Two incoherent point sources are imaged by that system. For simplicity, we consider them to have equal intensities and to be located at two unknown points $X_\pm=\pm d$ of the object plane. The task is to give a sensible estimate of the separation $\delta=X_+-X_-$. The relevant density matrix, which embodies the image-plane modes, can be jotted down as

$$\rho_d=\tfrac{1}{2}(|\psi_+\rangle\langle\psi_+|+|\psi_-\rangle\langle\psi_-|)\,, \tag{1}$$

where $|\psi_\pm\rangle=\exp(\pm idP)|\psi\rangle$, and P is the momentum operator that generates displacements in the x variable. In the x-representation, ρ_d appears as the normalized mean intensity profile, which is the image of spatially-shifted PSFs; namely, $\rho_d(x)=\frac{1}{2}(|\psi(x-d)|^2+|\psi(x+d)|^2)$. This confirms that the momentum acts as a derivative $P=-i\partial_x$, much in the same way as in quantum optics.

For points close enough together ($d\ll 1$), which we shall asume henceforth, a linear expansion gives

$$|\psi_\pm\rangle=\mathscr{N}\,(1\pm idP)\,|\psi\rangle\,, \tag{2}$$

where $\mathscr{N}=[1+d^2\langle\psi|P^2|\psi\rangle]^{-1/2}$ is a normalization constant. The crucial point is that $\langle\psi_-|\psi_+\rangle\neq 0$, so the spatial modes excited by the two sources are not orthogonal, in general. This overlap is at the heart of all the difficulties of the problem, for it implies that the two modes cannot be separated by independent measurements.

To bypass this problem, we bring in the symmetric and antisymmetric states

$$\begin{aligned}|\psi_s\rangle&=C_s(|\psi_+\rangle+|\psi_-\rangle)\simeq|\psi\rangle\,,\\ |\psi_a\rangle&=C_a(|\psi_+\rangle-|\psi_-\rangle)\simeq\frac{P|\psi\rangle}{\sqrt{\langle\psi|P^2|\psi\rangle}}\,,\end{aligned} \tag{3}$$

where C_a and C_s are normalization constants. When $\langle\psi|P|\psi\rangle=0$, these modes are orthogonal. This happens when; for example, the PSF is inversion symmetric, which

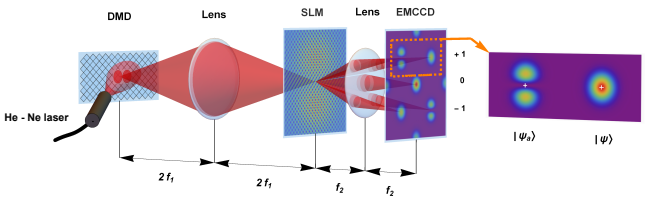

FIG. 1. Schematic diagram of the experimental setup. Two incoherent point sources are created with a high frequency switched digital micromirror chip (DMD) illuminated with an intensity stabilized He-Ne laser. The sources are imaged by a low-aperture lens. In the image plane, projection onto different modes is performed with a digital hologram created with an amplitude spatial light modulator (SLM). Information about the desired projection is carried by the first-order diffraction spectrum, which is mapped by a lens onto a EMCCD camera.

encompasses most of the cases of interest. The modes in (3) constitute a natural set for writing the density operator. Actually, in this set ρ_d is diagonal $\rho_d|\psi_j\rangle = p_j|\psi_j\rangle$, with eigenvalues $p_a = d^2\langle\psi|P^2|\psi\rangle$ and $p_s = 1-p_a$.

As we are estimating the separation δ, the pivotal quantity is the quantum Fisher information [14]. It is defined as $\mathscr{F} = \mathrm{Tr}[\rho_d L_d^2]$, where the symmetric logarithmic derivative L_d is the selfadjoint operator satisfying $\frac{1}{2}(L_d\rho_d + \rho_d L_d) = \partial\rho_d/\partial d$ [15]. A direct calculation finds that

$$\mathscr{F} = 2\left[\frac{1}{p_a}\langle\psi_a|\frac{\partial\rho_d}{\partial d}|\psi_a\rangle + \frac{1}{p_s}\langle\psi_s|\frac{\partial\rho_d}{\partial d}|\psi_s\rangle\right] \simeq \langle\psi|P^2|\psi\rangle\,, \tag{4}$$

and $\mathscr{F}$ turns out to be independent of d.

The qCRLB ensures that the variance of any unbiased estimator $\hat{\delta}$ of the quantity δ is then bounded by the reciprocal of the Fisher information; viz,

$$(\Delta\hat{\delta})^2 \geq \frac{1}{\mathscr{F}} = \frac{1}{\langle\psi|P^2|\psi\rangle}\,. \tag{5}$$

As this accuracy remains also constant, considerable improvement can be obtained if an optimal quantum measurement, saturating (5), is implemented.

Before we proceed further, we make a pertinent remark. The classical Fisher information for this problem reads as

$$\mathscr{F}_{\mathrm{cl}} = \int_{-\infty}^{\infty}\frac{1}{\rho_d(x)}\frac{\partial^2\rho_d(x)}{\partial d^2}\,\mathrm{d}x\,. \tag{6}$$

Performing again a first-order expansion in d, $\mathscr{F}_{\mathrm{cl}}$ can be expressed in terms of the PSF $I(x)$:

$$\mathscr{F}_{\mathrm{cl}} \simeq d^2\int_{-\infty}^{\infty}\frac{[I''(x)]^2}{I(x)}\,\mathrm{d}x\,. \tag{7}$$

Now, $\mathscr{F}_{\mathrm{cl}}$ goes to zero quadratically as $d\to 0$. This means that, in this classical strategy, detecting intensity at the image plane is progressively worse at estimating the separation for closer sources, to the point that the classical CRLB diverges at $d=0$. This divergent behavior has been termed the *Rayleigh's curse* [11]. In other words, there is much more information available about the separation of the sources in the phase of the field than in the intensity alone.

From our previous discussion, it is clear that the projectors $\Pi_j = |\psi_j\rangle\langle\psi_j|$ $(j=a,s)$ comprise the optimal measurements of the parameter d. Notice that in Eq. (4), the antisymmetric mode p_a gives the leading contribution and thus most useful information can be extracted from the Π_a channel. As a consequence, the wave function of the optimal measurement becomes

$$\psi_{\mathrm{opt}}(x) = \langle x|\psi_a\rangle = \frac{\psi'(x)}{\sqrt{\mathscr{F}(x)}} \tag{8}$$

where the x representation of the quantum Fisher information is

$$\mathscr{F}(x) = \langle\psi|P^2|\psi\rangle = \int_{-\infty}^{\infty}[\psi'(x)]^2\,\mathrm{d}x\,. \tag{9}$$

Let us consider two relevant examples of PSFs; the Gaussian and the sinc:

$$\psi^G(x) = \frac{1}{(2\pi\sigma^2)^{\frac{1}{4}}}\exp\left(-\frac{x^2}{4\sigma^2}\right), \quad \psi^s(x) = \frac{1}{\sqrt{w}}\mathrm{sinc}\left(\frac{\pi x}{w}\right), \tag{10}$$

where σ and w are effective widths that depend on the wavelength. From Eq. (9) it is straightforward to obtain the quantum Fisher information for these two cases: $1/(4\sigma^2)$ and $\pi^2/(3w^2)$, respectively. The optimal measurements are then

$$\psi^G_{\mathrm{opt}}(x) = \frac{1}{(2\pi)^{\frac{1}{4}}\sigma^{\frac{3}{2}}}x\exp\left(-\frac{x^2}{4\sigma^2}\right),$$
$$\psi^S_{\mathrm{opt}}(x) = \sqrt{3}\left[\frac{w^{\frac{1}{2}}}{\pi x}\cos\left(\frac{\pi x}{w}\right) - \frac{w^{\frac{3}{2}}}{\pi^2x^2}\sin\left(\frac{\pi x}{w}\right)\right]. \tag{11}$$

To project on these functions, one needs to separate the image-plane field in terms of the desired spatial modes. This has been implemented in our laboratory with the setup sketched in Fig. 1. Two incoherent point-like sources were generated by a Digital Light Projector (DLP) Lightcrafter evaluation module (Texas Instruments), which uses a digital micromirror chip (DMD) with square micromirrors of 7.6 μm size each. This allows for a precise control of the points separation by individually addressing two particular micromirrors. The DMD chip was illuminated by an intensity-stabilized He-Ne laser equipped with a beam expander to get a sufficiently uniform beam. The spatial incoherence is ensured by switching between the two object points, so that only one was ON at a time, keeping the switching time well below the detector time resolution.

The two point sources were imaged by a low numerical-aperture lens and shaped by an aperture placed behind the lens. A circular diaphragm produced Airy rings, but these are well approximated by a Gaussian PSF. The sinc PSF was obtained by inserting a squared slit. We experimentally measured the values $\sigma = 0.05$ mm and $w = 0.15$ mm. The

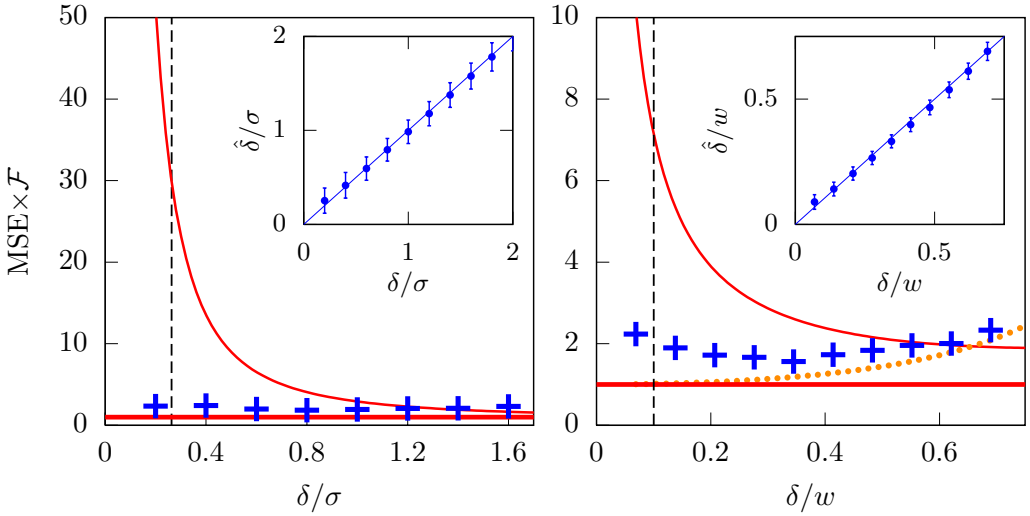

FIG. 2. Mean-square error (MSE) of the estimated separation for Gaussian (left panel) and sinc (right panel) PSFs. Separations are expressed in units of PSF widths σ and w and the MSE in units of the qCRLB. The main graph compares the performance of our experimental method (blue symbols) with the theoretical lower bound for the CCD measurement (thin red curve) and the ultimate quantum limit (thick red line). The vertical dotted lines delimit the 10% of the Rayleigh limit for each PSF. The insets show the statistics of the experimental estimates. Mean values are plotted in blue dots with standard deviation bars around. The true values are inside the standard deviation intervals for all separations and the estimator bias is negligible. For the two largest measured separations, the experimental MSE nicely follows the classical CRLB calculated for the experimentally realized antisymmetric projection (orange dots).

Rayleigh criterion for these values are 2.635σ and w, respectively. The two-point separations δ were varied in steps of 0.01 mm, which corresponds to steps 0.2σ for the Gaussian and $0.067w$ for the sinc. The smallest separations attained are 13 times smaller than the Rayleigh limit for the Gaussian and 10 times for the sinc.

The projection onto any basis is performed with a spatial light modulator (CRL OPTO) in the amplitude mode. We prepare a hologram at the image plane produced as an interference between a tilted reference plane wave and the desired projection function $\psi_{\rm opt}$. When this is illuminated by the two-point source, the intensity in the propagation direction of the reference wave is

$$\left|\int_{-\infty}^{\infty}\psi_{\rm opt}^{*}(x)\,\psi(x+d)\,{\rm d}x\right|^{2}+\left|\int_{-\infty}^{\infty}\psi_{\rm opt}^{*}(x)\,\psi(x-d)\,{\rm d}x\right|^{2}. \tag{12}$$

Different projections can be obtained with different reference waves.

To prepare the hologram, nominal PSF parameters (σ and w) were measured in advance. For the Gaussian PSF, we prepared projection on both the zeroth- and first-order Hermite-Gaussian modes. The measurement of the zeroth-order mode is used to assess the total number of photons in each measurement run. For the sinc, the image was also projected on the PSF itself and its first spatial derivative.

The desired projection is carried by the first diffraction order. To get the information, the signal is Fourier transformed by a short-focal lens and detected by a cooled electron-multiplying CCD (EMCCD) camera (Raptor Photonics) working in the linear mode with on-chip gain to suppress the effects of read-out noise and dark noise. As sketched in Fig. 1, the outcome of a measurement consists of two photon counts detected from the Fourier spectrum points representing spatial frequencies connected with the reference waves. This data carries information about the separation of the two incoherent point sources.

The excess noise of EMCCD gain g constitutes a remaining noise source. The numbers of photons n_0 and n_a detected in the PSF $|\psi\rangle$ and antisymmetric (optimal) modes $|\psi_a\rangle$, respectively, was determined by using the EMCCCD pixel capacity and g. The relative frequency of measuring the antisymmetric projection was calculated as $f_a = n_a/(n_0+n_a)$, the denominator n_0+n_a being roughly the total number of detected photons. The estimator of the separation is then obtained by solving the relation $f_a = \langle\psi_a|\rho_d|\psi_a\rangle$ for d. In doing so we make no assumption about the smallness of δ, which helps to produce unbiased estimates of larger separations.

To determine estimator characteristics, 500 measurements for each separation were carried out. Results are sumarized on the Fig. 2. The optimal method overcomes the direct position measurement for small and moderate separations. For the Gaussian PSF (left panel) and the smallest separation 0.2σ, the experimental mean squared estimator (MSE) is $2.35\times$qCRLB; i.e., more than 20 times smaller than the er-

ror of the position measurement (51.2×qCRLB). For the sinc, the experimental MSE is 2.23×qCRLB for the smallest separation, which is 4.5 times lower than the error of the position measurement (10.1×qCRLB). We mention in passing that the optimal measurement of the sinc PSF is more challenging due to very fast oscillations of the PSF derivative. Nevertheless, the results are quite satisfactory good and in complete agreement with the theory.

In summary, we have developed and demonstrated a simple technique that surpasses traditional imaging in its ability to resolve two closely spaced point sources. The method does not require any exotic illumination and is applicable to classical incoherent sources. Much in the spirit of the original proposal [11–13], our results stress that diffraction resolution limits are not a fundamental constraint but, instead, the consequence of traditional imaging techniques discarding the phase information present in the light.

Moreover, our treatment also suggests other directions of research. Whereas the point source represents a natural unit for image processing (upon which hinges the very definition of PSF), other "quantum units" can be further expanded and processed in a similar way. Optimal detection can then be tailored to suit the desired target. We have shown this for two particular cases of projections. This clearly provides a novel and not yet explored avenue for image processing protocols. We firmly believe that this approach will have a broad range of applications in the near future.

Note: While preparing this manuscript, we came to realize that similar conclusions, although with different techniques, were being reached by Sheng *et al* [16], Yang *et al* [17], and Tham *et al* [18].

FUNDING INFORMATION

We acknowledge financial support from the Technology Agency of the Czech Republic (Grant TE01020229), the Grant Agency of the Czech Republic (Grant No. 15-03194S), the IGA Project of the Palacký University (Grant No. IGA PrF 2016-005) and the Spanish MINECO (Grant FIS2015-67963-P).

ACKNOWLEDGMENTS

We thank Gerd Leuchs, Robert Boyd, Juan J. Monzón, Olivia Di Matteo, and Matthew Foreman for valuable discussions and comments.

[1] E. Abbe, Arch. Mikrosk. Anat. **9**, 469 (1873).
[2] J. W. Goodman, *Introduction to Fourier Optics* (Roberts and Company, Englewood, 2004).
[3] L. Rayleigh, Phil. Mag. **8**, 261 (1879).
[4] Focus issue: Super-resolution Imaging, Nat. Photonics **3**, 361 (2009).
[5] S. W. Hell, Science **316**, 1153 (2007).
[6] M. I. Kolobov, *Quantum Imaging* (Springer, Berlin, 2007), chap. Quantum Limits of Optical Super-Resolution, pp. 113–138.
[7] S. W. Hell, Nat. Meth. **6**, 24 (2009).
[8] G. Patterson, M. Davidson, S. Manley, and J. Lippincott-Schwartz, Annu. Rev. Phys. Chem. **61**, 345 (2010).
[9] A. J. den Dekker and A. van den Bos, J. Opt. Soc. Am. A **14**, 547 (1997).
[10] C. Cremer and B. R. Masters, Eur. Phys. J. H **38**, 281 (2013).
[11] M. Tsang, R. Nair, and X.-M. Lu, arXiv:1511.00552
[12] R. Nair and M. Tsang, arXiv: 16004.00937
[13] S. Z. Ang, R. Nair, and M. Tsang, arXiv:1606.00603
[14] L. Motka, B. Stoklasa, M. D'Angelo, P. Facchi, A. Garuccio, Z. Hradil, S. Pascazio, F. V. Pepe, Y. S. Teo, J. Rehacek, and L. L. Sanchez-Soto, Eur. Phys. J. Plus **131**, 130 (2016).
[15] D. Petz and C. Ghinea, *Introduction to Quantum Fisher Information* (World Scientific, 2011), vol. Volume 27, pp. 261–281.
[16] T. Z. Sheng, K. Durak, and A. Ling, arXiv:1605.07297
[17] F. Yang, A. Taschilina, E. S. Moiseev, C. Simon, and A. I. Lvovsky, arXiv:1606.02662
[18] W. K. Tham, H. Ferretti, and A. M. Steinberg, arXiv:1606.02666